

Received May 10, 2020, accepted May 22, 2020, date of publication May 26, 2020, date of current version June 9, 2020.

Digital Object Identifier 10.1109/ACCESS.2020.2997727

# An Adaptive and Flexible Brain Energized Full Body Exoskeleton With IoT Edge for Assisting the Paralyzed Patients

SUNIL JACOB<sup>1,2</sup>, (Member, IEEE), MUKIL ALAGIRISAMY<sup>3</sup>,  
VARUN G. MENON<sup>4</sup>, (Senior Member, IEEE), B. MANOJ KUMAR<sup>5</sup>, N. Z. JHANJHI<sup>6</sup>,  
VASAKI PONNUSAMY<sup>7</sup>, P. G. SHYNU<sup>8</sup>, AND VENKI BALASUBRAMANIAN<sup>9,10</sup>, (Member, IEEE)

<sup>1</sup>Department of Electronics and Communication Engineering, Lincoln University College, Petaling Jaya 47301, Malaysia

<sup>2</sup>Department of Electronics and Communication Engineering, SCMS School of Engineering and Technology, Ernakulam 683576, India

<sup>3</sup>Department of Electrical and Electronics and Engineering, Lincoln University College, Petaling Jaya 47301, Malaysia

<sup>4</sup>Department of Computer Science and Engineering, SCMS School of Engineering and Technology, Ernakulam 683576, India

<sup>5</sup>Department of Automobile Engineering, SCMS School of Engineering and Technology, Ernakulam 683576, India

<sup>6</sup>School of Computer Science and Engineering, Taylor's University, Subang Jaya 47500, Malaysia

<sup>7</sup>Faculty of Information and Communication Technology, Universiti Tunku Abdul Rahman, Kampar 31900, Malaysia

<sup>8</sup>School of Information Technology and Engineering, Vellore Institute of Technology, Vellore 632014, India

<sup>9</sup>School of Science, Engineering and Information Technology, Federation University, Mount Helen, VIC 3350, Australia

<sup>10</sup>Anidra Tech Ventures Pvt Ltd., Wyndham Vale, VIC 3024, Australia

Corresponding authors: Sunil Jacob (sunil@scmsgroup.org) and Vasaki Ponnusamy (vasaki@utar.edu.my)

This work was supported in part by the Institute of Electrical and Electronics Engineers (IEEE) EPICS, USA, under Grant 2016-12.

**ABSTRACT** The paralyzed population is increasing worldwide due to stroke, spinal cord injury, post-polio, and other related diseases. Different assistive technologies are used to improve the physical and mental health of the affected patients. Exoskeletons have emerged as one of the most promising technology to provide movement and rehabilitation for the paralyzed. But exoskeletons are limited by the constraints of weight, flexibility, and adaptability. To resolve these issues, we propose an adaptive and flexible Brain Energized Full Body Exoskeleton (BFBE) for assisting the paralyzed people. This paper describes the design, control, and testing of BFBE with 15 degrees of freedom (DoF) for assisting the users in their daily activities. The flexibility is incorporated into the system by a modular design approach. The brain signals captured by the Electroencephalogram (EEG) sensors are used for controlling the movements of BFBE. The processing happens at the edge, reducing delay in decision making and the system is further integrated with an IoT module that helps to send an alert message to multiple caregivers in case of an emergency. The potential energy harvesting is used in the system to solve the power issues related to the exoskeleton. The stability in the gait cycle is ensured by using adaptive sensory feedback. The system validation is done by using six natural movements on ten different paralyzed persons. The system recognizes human intentions with an accuracy of 85%. The result shows that BFBE can be an efficient method for providing assistance and rehabilitation for paralyzed patients.

**INDEX TERMS** Artificial intelligence, assistive technologies, brain-computer interface, edge computing, Internet of Things (IoT), rehabilitation.

## I. INTRODUCTION

A recent survey carried out by Toyota Foundations revealed that 30% of the paralyzed population is disappointed with the assistive devices in the market. The outdated design of assistive devices is causing constant pain and frustration. Survey participants also recommended that future assistive

The associate editor coordinating the review of this manuscript and approving it for publication was Zhenyu Zhou<sup>10</sup>.

devices should be easy to handle and help in daily activities. The respondents also indicated that the design should be natural, like an extension of their body, providing them freedom and independence [1], [2]. Currently, exoskeletons are the most popular solution used in rehabilitation and assistance of the paralyzed people [3]–[8]. Numerous types of exoskeletons are designed for purposes ranging from rehabilitation and assistance to transportation and handling heavy load in industries.

In rehabilitation, the exoskeletons are used to work in parallel with the human legs and carry out the desired actions with ease. These devices are specifically designed to treat disabilities of patients in a clinical setting. The rehabilitation exoskeleton helps paralyzed patients to engage with real-world things and to monitor the movement of body parts. Exoskeletons are also designed for healthy subjects, enabling them to interact with a virtual environment [9]. As healthy people use these haptic exoskeletons, ease of wearability is not a major issue, but portability and efficient finger tracking are highly required. In recent times, to assist children having cerebral palsy disorders, exoskeletons have been designed [10]. The architecture of the control unit, the mechanical system, and feature extraction is discussed in detail. In [11], a wearable hip assist robot is discussed, which is used to improve the gait function and reduce muscle effort and metabolic activities. The device can reduce knee and ankle muscle activity along with a decrease in hip movements. The robot can stabilize the trunk during walking in adults. But the system has not investigated the effectiveness of gait rehabilitation.

In [12], the translation of gait without using crutches gait in a biped robot is demonstrated. The mathematical hybrid model analysis is carried out to find different gait and walking speeds. The walking gaits are stabilized using a centralized controller. A knee exoskeleton that can be used for sit to stand assistance is discussed in [13]. Here, the torque control is improved using a unique transmission configuration, also with reduced output impedance. Design specifications of the current lower limb exoskeletons are reviewed, and the human biomechanical consideration in lower limb design is analyzed in [14]. The classification and design challenges in the field of Exoskeleton and Orthoses are discussed in [15]. In [16], the classification of exoskeletons into the palm, upper limb, and lower limb exoskeleton is discussed. Further, the paper discusses various exoskeletons proposed for rehabilitation and enhancement purposes. The paper also puts forward the concept of developing a full-body exoskeleton.

In [17], a wearable full-body exoskeleton is designed for a mobile cyber-physical system. Here, the design of a new technique for identifying the gate phase is also discussed. Energy harvesting using human's daily actions is proposed to charge the battery of exoskeleton in [18]. Conventional and alternative methods for providing power to exoskeletons are discussed. A systematic review of various types of exoskeletons for using with the lower limb in neurorehabilitation is presented in [19]. In [20], an exoskeleton to aid patient rehabilitation with postural equilibrium is designed. Multi-variable robust control with the patient's Electro Myographical (EMG) signals is utilized to achieve equilibrium. Berkeley Lower Limb Exoskeleton (BLEEX) [21] is designed to transfer load and body weight into the ground, which reduces the metabolic cost of the wearer. This parallel exoskeleton is able to enhance the endurance of the user. The exoskeleton, which augments the torque and power of the user during lifting and daily activities, is discussed.

Software-Defined Network (SDN) assisted solutions with exoskeletons for use in rehabilitation are also proposed recently [22]. The majority of the existing exoskeletons have weight, flexibility, and adaptability constraints. Easy wearability and portability are other significant limitations experienced by current assistive exoskeleton-based solutions for rehabilitation [23]–[25].

To overcome the current issues existing with exoskeletons, we propose an adaptive and flexible Brain Energized Full Body Exoskeleton (BFBE) for assisting the paralyzed people. In the BFBE system, the brain signals captured by the EEG sensors are used for controlling the movements of the exoskeleton. The flexibility is incorporated into the system by a modular design approach. The BFBE system has a BCI module, a Control Unit (CU), and a Body-Part Actuation Module (BAM). BCI module captures the brain signal and transforms it into a signal that can be used by the CU. The processing happens at the edge, thus reducing delay in decision making, and the system is further integrated with an IoT module that helps to send an alert message to multiple caregivers in case of an emergency. The system is non-invasive, and the fabricated EEG sensor is used to collect the signals from the scalp. An instrumentation amplifier is used to enhance the strength of the obtained signals. The output signal from the amplifier is subjected to filtering and pre-processing. The signals are generated for different basic human actions (sitting, standing, sleeping) and then after the pre-processing is stored in a database. When the paralyzed person has an intention to make a particular movement, the microcontroller in the CU uses this database and produces the signal for activating the particular body part. The generated EEG pattern of the person is mapped into the corresponding action. The BAM then uses the motor driver circuit to pass the activation signal to the corresponding part of the body. The potential energy harvesting is used in the system to solve the power issues related to the exoskeleton. The stability in the gait cycle is ensured by using adaptive sensory feed-back.

The paper is arranged into 4 sections. The proposed work is discussed in Section 2. The system architecture is discussed initially, and then the theoretical analysis is presented. Section 3 presents and discusses the system working and testing details and the results obtained. Finally, the paper concludes in section 4. The list of abbreviations is listed in table 1.

## II. PROPOSED SYSTEM

### A. SYSTEM ARCHITECTURE

The architecture of the Brain Energized Full Body Exoskeleton (BFBE) system is shown in Figure 1. The BFBE system has three major modules 1) BCI module, 2) Control Unit, and 3) Body-Part Actuation Module. The primary function of the BCI module is to collect the EEG signals from the scalp and then convert it into a form that can be used by the CU. We have fabricated a sixteen-electrode based EEG sensor, which is used in the proposed system for collecting the signals and also for analyzing the brain activity. For removing the

TABLE 1. List of abbreviations.

Abbreviation	Description
BFBE	Brain Energized Full Body Exoskeleton
DoF	Degrees of Freedom
EEG	Electroencephalogram
EMG	Electro Myographical
BLEEX	Berkeley Lower Limb Exoskeleton
SDN	Software-Defined Network
CU	Control Unit
BAM	Body-Part Actuation Module
IoT	Internet of Things
BCI	Brain Computer Interface
WHT	Walsh Hadamard Transform

TABLE 2. Body parts of BFBE and its corresponding joints.

Different modules of the exoskeleton	Joints used to control the movements
Lower limb (Left & Right)	Knee Joint Left, Foot Joint Left, Knee Joint Right, Foot Joint Right
Upper limb (Left & Right)	Elbow Joint Right, Elbow Joint Left, Hand Joint Left, Hand Joint Right
Head & Neck	Head Joint, Neck Joint
Shoulder (Left & Right)	Shoulder Joint Left, Shoulder Joint Right
Hip	Torso Joint, Hip Joint Left, Hip Joint Right
Lower limb (Left & Right)	Knee Joint Left, Foot Joint Left, Knee Joint Right, Foot Joint Right

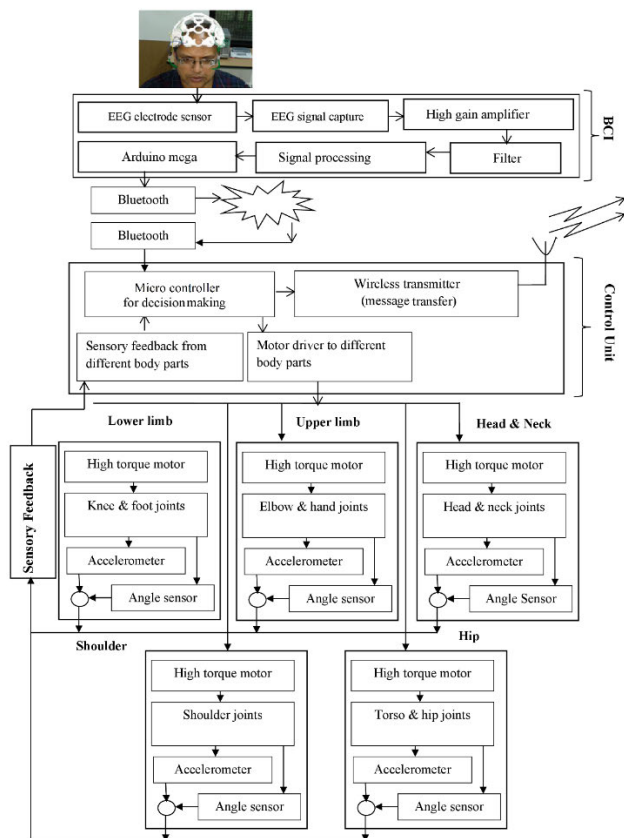


FIGURE 1. System architecture: Brain Energized Full Body Exoskeleton (BFBE).

high-frequency noise, we use a bandpass. Walsh Hadamard Transform (WHT) is then used to transform the signals into the frequency domain.

The signals are further transformed into a digital form and provided to the Arduino Mega, which transmits the signal via Bluetooth to the Control Unit. The signals are generated for different basic human actions (sitting, standing, sleeping) and then after the pre-processing is stored in a database. When the paralyzed person has an intention to make a particular movement, the microcontroller in the CU uses this

database and produces the signal for activating the particular part of the body. The generated EEG pattern of the person is mapped into the corresponding action. The BAM then uses the motor driver circuit to pass the activation signal to the corresponding part of the body. The potential energy harvesting is used in the system to solve the power issues related to the exoskeleton. The stability in the gait cycle is ensured by using adaptive sensory feed-back. The feedback to the CU is provided using a multi-level sensing technique so that corrections can be made in the process. Required corrections for producing the actuation signals are done by the microcontroller using this feedback and thus improving the decision-making accuracy. An accelerometer is used on the backside for detecting accidental falls. The processing happens at the edge, thus reducing delay in decision making, and the system is further integrated with an IoT module that helps to send an alert message to multiple caregivers in case of an emergency. If the measured tilt passes a particular threshold, a similar emergency message will be given to the caregiver via a wireless transmitter. The secure communication is ensured between paralyzed persons and caregivers using a double encrypted NTSA algorithm [26]. The material used for the development is carbon fiber, so that it can easily replicate various body movements with ease. The BFBE has a total of 15 degrees of freedom spread across different joints of the body, as indicated in Table 2.

Each of these joints is realized using high torque motors. Controlling the angle of rotation of the motors enables the system to make different movements. The exoskeleton is easy to wear due to its flexible and detachable components. The straps are used to tie the exoskeleton to different body parts. To further improve the stability of the person, support is provided on the backside and ankle region. In order to check if the applied force is sufficient to make the exoskeleton stable, angle sensors are placed on the joints.

**B. SYSTEM DESIGN AND METHODOLOGY**

The full-body structure of the exoskeleton mainly consists of five different body parts, which are lower limb, upper limb, head & neck, shoulder, and hip. The BFBE structured is designed by integrating these parts. The modular design provides BFBE with the highly required flexibility. The system can thus be used by people with different degrees of paralysis.

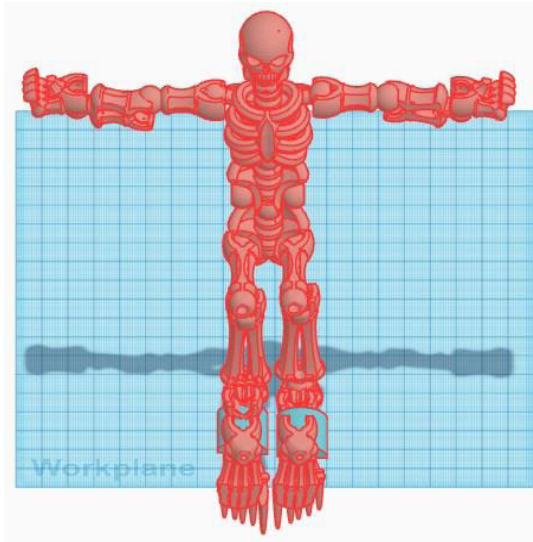


FIGURE 2. Sitting posture of BFBE (3D model).

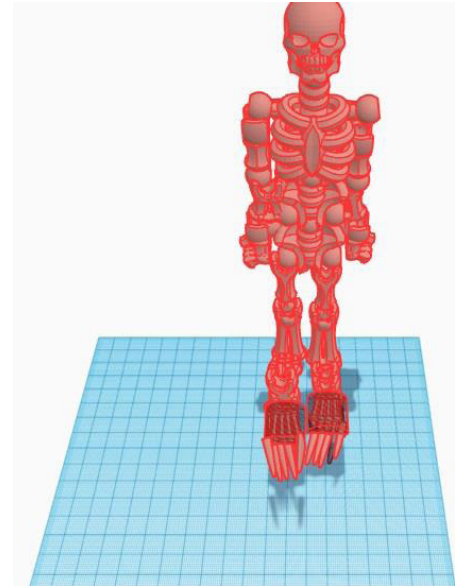


FIGURE 3. Standing posture of BFBE (3D model).

1) EXOSKELETON DESIGN FOR DIFFERENT POSTURES

In this section, we discuss the design generated for the exoskeleton in different body postures. BFBE exoskeleton is constructed to mirror the anatomy of the human body. Figure 2 illustrates the full-body exoskeleton designed using 3D software to emulate sitting posture. The major advantage of the exoskeleton system is that the various parts and the joints can be attached and detached easily. The system can thus be used by people with different degrees of paralysis. The full-body exoskeleton can be used by a completely paralyzed person. paralysis can be provided with a customized exoskeleton. People experience the ease of wearability and mobility because of the development of the exoskeleton with carbon fiber material. To further improve the stability of the person, on the backside and in the ankle region, a support is provided with the system. Actuating the motors placed at the corresponding joints helps to move from sleeping to the sitting posture.

Figure 3 shows the standing posture of the full-body exoskeleton. The system translates from sleeping to standing based on the acquired human intentions. The high torque motors placed at the different joints help in lifting the human weight. If the actuation signals produced are not sufficient, more accurate signals will be generated based on the feedback received. A customized execution pattern is used to maintain stability and reduce errors. The design also ensures that no direct transition from sleeping to standing or vice versa.

III. MATHEMATICAL ANALYSIS OF THE PROPOSED SYSTEM

The mathematical analysis is done on the full-body exoskeleton to identify the desired torque proportional to the mass. The joints used to provide 15 degrees of freedom are utilized to control the different bones of the human skeleton. Figure 4 presents the exoskeleton structure used for the analysis. Here, *A* is the head joint (HJ), *b* is the neck joint (NJ),

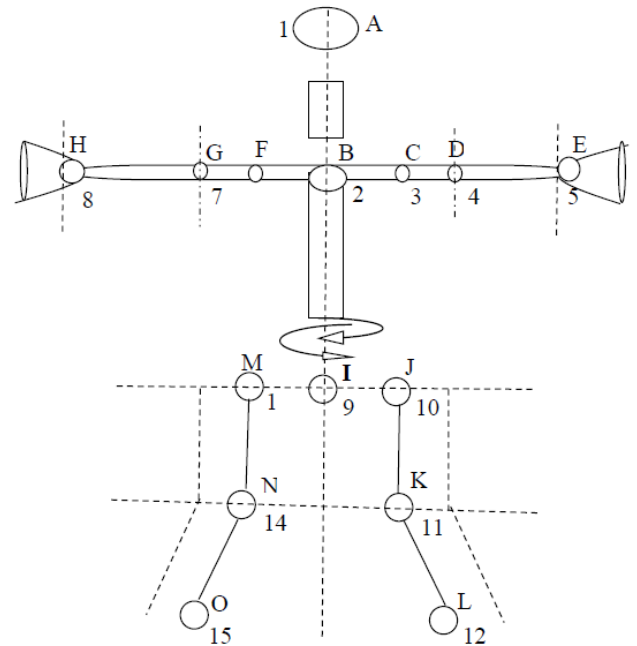


FIGURE 4. Exoskeleton structure used for analysis.

*c* is the left shoulder joint left (SJL), *d* is the elbow joint left (EJL), *e* is the hand joint left (HJL), *f* is the shoulder joint right (SJR), *g* is the elbow joint right (EJR), *h* is the hand joint right (HJR), *lr* and *lh* are the links for humanoid limbs.

Let the angle of the limb with respect to vertical and horizontal axis is denoted by ' $\theta$ ', the masses of the element by *m<sub>i</sub>*, the length of the elements by *l<sub>i</sub>*, and the center of gravity of the system by *G<sub>i</sub>*. The spring of the element is represented by spring coefficient *K<sub>i</sub>*. The angles are referenced with horizontal and vertical axis where *L* denotes the kinetic and *P* denotes

the potential energy, and  $\in$  is the force to be applied to the joint.

Let the different control signals to be applied at hip and knee joint of human and exoskeleton be defined as  $\hat{A}$  for the angular acceleration of knee,  $\hat{\dot{A}}$  for the angular velocity of the knee,  $\hat{A}$  for the angular position of the knee,  $\hat{J}$  for the total torque applied on the knee and the ankle,  $\hat{I}$  for the inertia on the foot and the shank. Let the length of the shank is  $\hat{L}m$ , length of the foot is  $\hat{L}m$ , the mass of the shank is  $\hat{O}$  kg, mass of the foot is  $\hat{O}$  kg and let the torque be proportional to mass.

Consider the upper part of the body. The driving motor is located at the head joint driven by  $V_{HJ}$ ,  $V_{NJ}$  is the neck joint motor driving voltage,  $V_{SJL}$  is the shoulder joint left motor driving voltage,  $V_{SJR}$  is the shoulder joint right motor driving voltage. Because of the DC voltage, we have currents  $I_{HJ}$ ,  $I_{NJ}$ ,  $I_{SJL}$ ,  $I_{SJR}$ , entering the exoskeleton upper part. The current flowing from the neck joint to the head joint is denoted by  $I_{NH}$ . We have  $I_{NJ} = I_{NH}$ ,  $I_{SJL} = 0$ ,  $I_{SJR} = 0$ ,  $I_{HJ} = -I_{NH}$  and  $I_{NH} = S_M(V_{NJ}, V_{SJR}, V_{SJL}, V_{HJ})$ , where  $S_M$  is a function classified based on the portion at the exoskeleton. Also ' $\in$ ' is the force to be applied to the joint to move from an initial position or angle ' $\theta$ ' to final position angle ' $\theta'$ '. The length of the exoskeleton part be  $l_i$  and the width is  $w_i$  and the initial position of the exoskeleton is ' $x$ ' along the axis. The net force applied to the head joint movement will be,

$$\in_{HJ} = \int_0^{<\theta} \in_{HJ}^1 W_i dx \quad (1)$$

With  $\in^1$  as the force applied per unit area, the width  $W_i$  becomes constant, thus we have,

$$\in_{HJ} = W_i \int_0^{<\theta} \in_{HJ}^1 dx \quad (2)$$

Similarly, we obtain other values of force applied on shoulder joint left and shoulder joint right as,

$$\in_{SJL} = W_i \int_0^{<\theta} \in_{SJL}^1 dx \quad (3)$$

$$\in_{SJR} = W_i \int_0^{<\theta} \in_{SJR}^1 dx \quad (4)$$

We can say that the net force applied to the head joint, shoulder joint left and shoulder joint right movement as a function of different voltages given by,

$$\in_{HJ} = f_{HJ}(V_{NJ}, V_{SJL}, V_{SJR}, V_{HJ}) \quad (5)$$

$$\in_{SJL} = f_{SJL}(V_{NJ}, V_{SJL}, V_{SJR}, V_{HJ}) \quad (6)$$

$$\in_{SJR} = f_{SJR}(V_{NJ}, V_{SJL}, V_{SJR}, V_{HJ}) \quad (7)$$

If we consider a time-varying voltage  $V_{NJ}$ ,  $V_{SJL}$ ,  $V_{SJR}$ ,  $V_{HJ}$  to move the exoskeleton at any position at any time, the neck to head force, shoulder joint left and shoulder joint right, as a function of time  $t$  is given by,

$$\in_{NH}^{(t)} = f_{HJ}(V_{NJ}(t), V_{SJL}(t), V_{SJR}(t), V_{HJ}(t)) \quad (8)$$

$$\in_{SJL}^{(t)} = f_{SJL}(V_{NJ}(t), V_{SJL}(t), V_{SJR}(t), V_{HJ}(t)) \quad (9)$$

$$\in_{SJR}^{(t)} = f_{SJR}(V_{NJ}(t), V_{SJL}(t), V_{SJR}(t), V_{HJ}(t)) \quad (10)$$

Here ' $f$ ' is the function taking the time-varying force into consideration. Now we have current acting at shoulder joint left and shoulder joint right given by,

$$I_{SJL}(t) = \frac{d}{dt} \in_{SJL} \quad (11)$$

$$I_{SJR}(t) = \frac{d}{dt} \in_{SJR} \quad (12)$$

As the incoming current is equal to the outgoing current, we have,  $I_{NJ}(t) + I_{HJ}(t) = \frac{d}{dt} \in_{NH}$ . With  $I_{NJD}(t)$  as the initial position, we have  $I_{NJ}(t) = I_{\mu}(t) + I_{NJD}(t)$ ,  $I_{HJ}(t) = -I_{\mu}(t) + I_{HJD}(t)$  and  $I_{NJD}(t) + I_{HJD}(t) = \frac{d}{dt} \in_{NH}$ .

Here,  $I_{\mu}(t)$  is fully responsible for the exact movement at the exact time and  $I_{NJD}$  and  $I_{HJD}$  for the correct initial position. We can call them as the returned coordinates. If  $I_{NJD}(t)$  is causing the change in the movement of exoskeleton by an angle  $\theta'$  in the given time  $\Delta t$ , then  $I_{NJD}(t) = \frac{d}{dt} \in'_{\theta}$ , and if  $I_{HJD}(t)$  is causing the change in the movement of exoskeleton by  $\theta''$  in the given time  $\Delta t$ , then  $I_{HJD} = \frac{d}{dt} \in''_{\theta}$ .

Change in the variation between the neck and the head joint is given by  $\frac{d}{dt} \in'_{\theta} + \frac{d}{dt} \in''_{\theta} = \frac{d}{dt} \in_{NH}$  that is  $\in'_{\theta} + \in''_{\theta} = \in_{NH}$ . Assuming two different movement angle force at  $<\theta'$  and  $<\theta''$  we have the force, variations given by,

$$\in'_{\theta'} = W_i \int_0^{<\theta'} \frac{x}{l_i} \in'_{HJ} dx \quad (13)$$

$$\in''_{\theta''} = W_i \int_0^{<\theta''} \left(1 - \frac{x}{l_i}\right) \in'_{HJ} dx \quad (14)$$

The net force applied is written as a function of different voltages given by,

$$\in'_{\theta'} = f_{\theta'}(V_{NJ}, V_{SJL}, V_{SJR}, V_{HJ}) \quad (15)$$

$$\in''_{\theta''} = f_{\theta''}(V_{NJ}, V_{SJL}, V_{SJR}, V_{HJ}) \quad (16)$$

Considering the time-varying voltage  $V_{NJ}$ ,  $V_{SJL}$ ,  $V_{SJR}$ ,  $V_{HJ}$  to move the exoskeleton at any position at any time, the neck to head force, shoulder joint left and shoulder joint right, as a function of time  $t$  is given by,

$$\in'_{\theta'}(t) = f_{\theta'}(V_{NJ}(t), V_{SJL}(t), V_{SJR}(t), V_{HJ}(t)) \quad (17)$$

$$\in''_{\theta''}(t) = f_{\theta''}(V_{NJ}(t), V_{SJL}(t), V_{SJR}(t), V_{HJ}(t)) \quad (18)$$

Considering the ' $f$ ' function takes time varying force into considerations, we have the current acting as,

$$I_{HJD}(t) = \frac{d}{dt} \in_{\theta'} \quad (19)$$

$$I_{HJD}(t) = \frac{d}{dt} \in_{\theta''} \quad (20)$$

$$I_{SJL}(t) = \frac{d}{dt} \in_{SJL} \quad (21)$$

$$I_{SJR}(t) = \frac{d}{dt} \in_{SJR} \quad (22)$$

The net current flowing through the exoskeleton is zero and given by,

$$I_{NJ}(t) + I_{HJ}(t) + I_{SJL}(t) + I_{SJR}(t) = 0 \quad (23)$$

$$I_{NJD}(t) + I_{HJD}(t) + I_{SJL}(t) + I_{SJR}(t) = 0 \quad (24)$$

Using the chain value of differentiation on the current values we obtain,

$$I_{NJD}(t) = \frac{\partial \epsilon_{\theta'}}{\partial V_{NJ}} \frac{d}{dt} V_{NJ} + \frac{\partial \epsilon_{\theta'}}{\partial V_{SJL}} \frac{d}{dt} V_{SJL} + \frac{\partial \epsilon_{\theta'}}{\partial V_{SJR}} \frac{d}{dt} V_{SJR} + \frac{\partial \epsilon_{\theta'}}{\partial V_{HJ}} \frac{d}{dt} V_{HJ} \quad (25)$$

$$I_{HJD}(t) = \frac{\partial \epsilon_{\theta''}}{\partial V_{NJ}} \frac{d}{dt} V_{NJ} + \frac{\partial \epsilon_{\theta''}}{\partial V_{SJL}} \frac{d}{dt} V_{SJL} + \frac{\partial \epsilon_{\theta''}}{\partial V_{SJR}} \frac{d}{dt} V_{SJR} + \frac{\partial \epsilon_{\theta''}}{\partial V_{HJ}} \frac{d}{dt} V_{HJ} \quad (26)$$

$$I_{SJL}(t) = \frac{\partial \epsilon_{SJL}}{\partial V_{NJ}} \frac{d}{dt} V_{NJ} + \frac{\partial \epsilon_{SJL}}{\partial V_{SJL}} \frac{d}{dt} V_{SJL} + \frac{\partial \epsilon_{SJL}}{\partial V_{SJR}} \frac{d}{dt} V_{SJR} + \frac{\partial \epsilon_{SJL}}{\partial V_{HJ}} \frac{d}{dt} V_{HJ} \quad (27)$$

$$I_{SJR}(t) = \frac{\partial \epsilon_{SJR}}{\partial V_{NJ}} \frac{d}{dt} V_{NJ} + \frac{\partial \epsilon_{SJR}}{\partial V_{SJL}} \frac{d}{dt} V_{SJL} + \frac{\partial \epsilon_{SJR}}{\partial V_{SJR}} \frac{d}{dt} V_{SJR} + \frac{\partial \epsilon_{SJR}}{\partial V_{HJ}} \frac{d}{dt} V_{HJ} \quad (28)$$

With  $dx$  as a small incremental moment for an incremental time  $d\tau$  we obtain,

$$dx = \frac{-K_i W_i}{\tilde{A}} \epsilon'_{HJ} d\tau \quad (29)$$

Substituting the above value of  $dx$  in (2) and (3) we obtain,

$$\epsilon_{SJL} = W_i \int_{\theta'}^{\theta''} \epsilon'_{SJL} \left( \frac{-K_i W_i}{\tilde{A}} \epsilon'_{HJ} d\tau \right) \quad (30)$$

$$\epsilon_{SJL} = \frac{-K_i W_i^2}{\tilde{A}} \int_{\theta'}^{\theta''} \epsilon'_{SJL} \epsilon'_{HJ} d\tau \quad (31)$$

$$\epsilon_{SJR} = \frac{-K_i W_i^2}{\tilde{A}} \int_{\theta'}^{\theta''} \epsilon'_{SJR} \epsilon'_{HJ} d\tau \quad (32)$$

$$\epsilon_{HJ} = \frac{-K_i W_i^2}{\tilde{A}} \int_{\theta'}^{\theta''} (\epsilon'_{HJ})^2 d\tau \quad (33)$$

Substituting the above value of  $dx$  in (12) and (13) we obtain,

$$\epsilon'_{\theta'} = \frac{-K_i W_i^2}{\tilde{A}} \int_{\theta'}^{\theta''} \frac{x}{l_i} (\epsilon'_{HJ})^2 d\tau \quad (34)$$

$$\epsilon''_{\theta''} = \frac{-K_i W_i^2}{\tilde{A}} \int_{\theta'}^{\theta''} \left( 1 - \frac{x}{l_i} \right) (\epsilon'_{HJ})^2 d\tau \quad (35)$$

Calculating 'x' in terms of torque we integrate 'x' from initial angle  $\theta'$  to final angle  $\theta''$ .

$$x = \frac{-K_i W_i}{\tilde{A}} \int_{\theta'}^{\theta''} \epsilon'_{HJ} d\tau \quad (36)$$

The  $V_{NJ}$  value for which we reach the maximum limit is  $V_{max}$ . If the value of  $V_{NJ}$  is raised above  $V_{max}$ , the exoskeleton movements will remain unaltered and practically constant. The human body parts will act as the dielectric of the capacitor with the exoskeleton acting as the plate of the capacitor. Here  $V_{OI}$  is the voltage applied between outer and inner exoskeleton,  $P_{limb}$  is the potential drop across the thickness of the limb,  $P_{IX}$  is the potential drop across the inner

surface of the exoskeleton, and  $P_{CM}$  is the potential at all the contact point across the exoskeleton and human limb. We now have,

$$VOJ = P_{limb} + PIX + PCM \quad (37)$$

The variation in the voltage is given by,  $\Delta V_{OJ} = \Delta P_{limb} + \Delta PIX + P_{CM}$  where,  $P_{CM}$  is constant.

Now there are three potential charges across the exoskeleton and the limb,  $\varphi_{OE}$  is the charge on the outer exoskeleton,  $\varphi_{limb}$  is the charge on the limb,  $\varphi_{IE}$  is the charge on the inner exoskeleton, and we have  $\varphi_{OE} + \varphi_{limb} + \varphi_{IE} = 0$  and  $\tilde{\varphi}_{OE} + \tilde{\varphi}_{limb} + \tilde{\varphi}_{IE} = 0$ . The charges per unit area are given by  $\Delta \tilde{\varphi}_{OE} + \Delta \tilde{\varphi}_{IE} = 0$  with  $\tilde{\varphi}_{limb}$  as constant.

To analyze the effect of external voltage on the exoskeleton, and the human limb, we are defining a threshold voltage depending on the EEG signal  $V_{th}$ . The minimum voltage required to trigger the movement is, if  $VOI < V_{th}$  then  $\tilde{\varphi}_{IE} > 0$  and  $PIX < 0$ , if  $VOI \geq V_{th}$  then  $\tilde{\varphi}_{IE} < 0$  and  $PIX > 0$ , if  $VOI = V_{th}$  then  $\tilde{\varphi}_{IE} = 0$  and  $PIX = 0$ . The signal from EEG headset to limb is defined as  $R_{surface-limb}$ ,  $ST$  is the potential depending on the thickness of limb, and  $LT$  is the length of the limb. The ratio of the potential drop across the inner surface of the exoskeleton to the length of the limb is given by  $P_{IX}/L_T$ . The signal transferred from EEG headset to the limb is given by,

$$R_{surface-limb} = S_T e^{P_{IX}/L_T} \quad (38)$$

The potential depending on the thickness of the limb is calculated as,

$$S_T = S_L e^{-P_{RX}/L_T} \quad (39)$$

Substituting the value of  $ST$  in (39), we obtain,

$$R_{surface-limb} = S_L e^{(P_{IX} - P_{RX})/L_T} \quad (40)$$

The capacitance coefficient variation in the direction of  $x$  and capacitance coefficient variation in the opposite direction of  $x$  given by,

$$K(x) = K_0 e^{P(x)/L_T} \quad (41)$$

$$K(y) = L_0 e^{-P(x)/L_T} \quad (42)$$

Potential is at its local maximum, which indicates that the system in the equilibrium state is unstable. We apply a small displacement to the exoskeleton and move it to a random small distance from its equilibrium state, and the total force of the exoskeleton makes it to move even farther. Mobility displacement along the  $x$  direction is given by,

$$\mu(x) = \vartheta (K(y) - K(x) - P_A) \quad (43)$$

$$\frac{d^2 P}{dy^2} = \frac{-\vartheta}{\mu_s} \left[ L_0 e^{-P(x)/L_T} - K_0 e^{P(x)/L_T} - P_A \right] \quad (44)$$

The charge on the inner skeleton is given by,

$$\tilde{\varphi}_{IE} = \frac{\mp \sqrt{2\vartheta \mu_s P_A} \sqrt{L_T e^{-P(x)/L_T} + P_{IX}}}{\sqrt{-L_T + e^{-P_{RX}/L_T} (L_T e^{P/L_T} - P_{IX} - L_T)}} \quad (45)$$

$$\tilde{\varphi}_{IE} = \tilde{C}_{limb} P_{limb} \quad (46)$$

$$\tilde{\varphi}_{IE} = -\sqrt{2\vartheta \mu_s P_A} \sqrt{P_{IX} + L_T e^{(P_{IX} - P_{RX})/L_T}} \quad (47)$$

$$\tilde{\varphi}_{IE} = \tilde{\varphi}_{RL} + \tilde{\varphi}_{SL} \quad (48)$$

The charge on the right-side outer skeleton to the limb is calculated as,

$$\tilde{\varphi}_{RL} = \int_{initial\theta}^{final} (\vartheta) K(x) (Adx) \quad (49)$$

The charge on the left-side outer skeleton to the limb is calculated as,

$$\tilde{\varphi}_{SL} = -\vartheta \int_{initial}^{final} K(x) dx \quad (50)$$

The body parameter constant with static exoskeleton movement is given by,

$$T_B = \sqrt{\frac{2\mu_s}{\vartheta P_A}} \sqrt{P_{IX}} \quad (51)$$

The small variation in the charge on the inner skeleton is given by,  $\Delta\tilde{\varphi}_{IE} = \Delta\tilde{\varphi}_{RL} + \Delta\tilde{\varphi}_{SL}$  where  $\tilde{\varphi}_{RL} = \tilde{\varphi}_{RL}(P_{IX})$  and  $\tilde{\varphi}_{SL} = \tilde{\varphi}_{SL}(P_{IX})$ . The voltage applied between the outer and inner exoskeleton is given by,

$$V_{OI} = V_{th} + P_{IX} - \frac{\tilde{\varphi}_{SL}(P_{IX}) + \tilde{\varphi}_{RL}(P_{IX})}{\tilde{limb}} \quad (52)$$

#### IV. RESULTS AND DISCUSSION

The designed system is tested on six different subjects, three healthy and three paralyzed persons. The collection of data is done in the offline and online phases. The experiments are carried out for three different human intentions like sleeping, standing, and sitting. To maintain stability, the movements are executed based on the designed pattern. In the offline training phase, the brain patterns corresponding to each of these intended movements are acquired using the 64 channel EEG sensor. Figure 5 presents the EEG Sensor manufactured with 16 Electrodes for collecting the signals.

Signal analysis is carried out using WHT, and the unique features required for the classification are extracted. Large amount of EEG signals is compressed using WHT, and a faster computation is also provided. The database is designed using the extracted information corresponding to each human thought obtained during the training phase. In the online phase, the WHT coefficients, along with extracted information, are transmitted from the brain to the full-body exoskeleton for the reconstruction of the original signal.

The EEG signals corresponding to human intentions of sitting and standing are depicted in figure 6. Here, the original signal and the reconstructed signal for both the postures are presented. Figure 7 shows the area matching of EEG patterns obtained for the sitting and standing postures. The original and reconstructed signal is correlated at the receiver side to identify the movement to be executed. Based on the classification results, the required joints are actuated to produce the desired movement by the exoskeleton system.



FIGURE 5. EEG sensor manufactured with 16 electrodes.

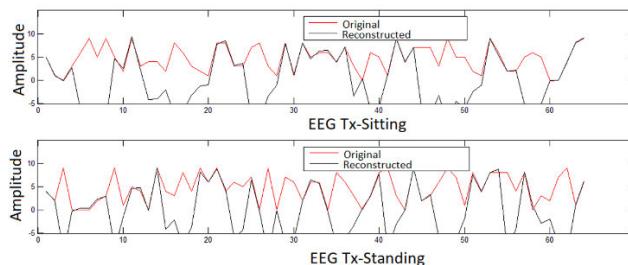


FIGURE 6. Original and reconstructed EEG signal in sitting and standing positions with BFBE.

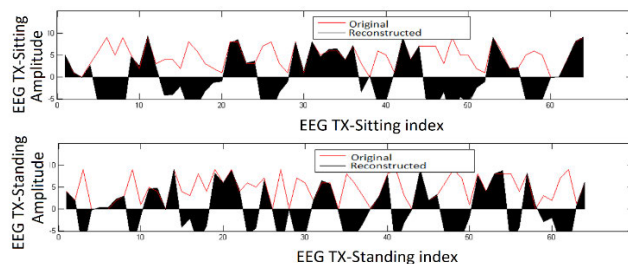


FIGURE 7. Area matching of EEG patterns obtained for sitting and standing posture.

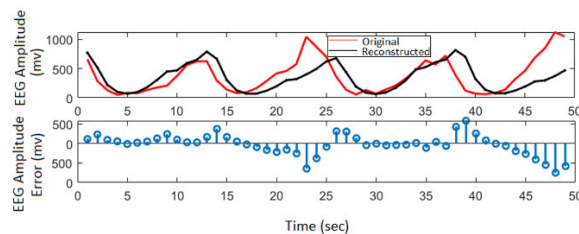


FIGURE 8. EEG amplitude and EEG amplitude error for original and reconstructed signals.

Figure 8 shows the varying of the EEG signal captured by the brain headset with time. The error in EEG amplitude for the signal is also shown in the figure. Figure 9 presents the brain pattern variations at different frequencies using the proposed system. The voltage spectral density variations at frequencies 6 Hz, 10 Hz and 22 Hz are presented and highlighted in the figure.

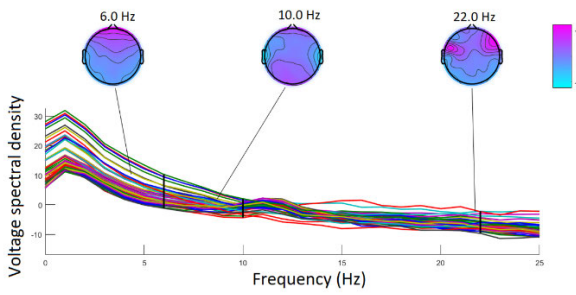


FIGURE 9. Brain pattern variations at different frequencies.

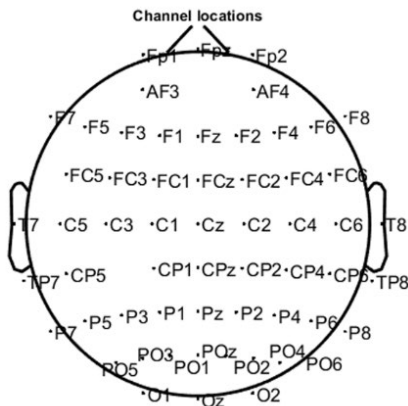


FIGURE 10. Electrode placement locations in the EEG headset.

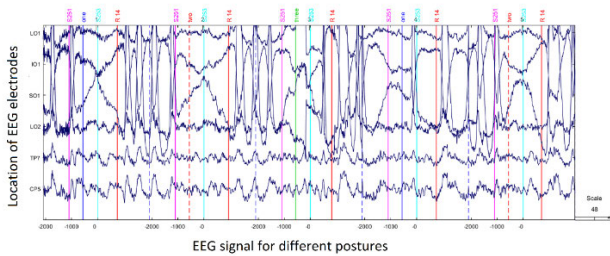


FIGURE 11. EEG for different postures with placement of electrodes from CP5 to LO1.

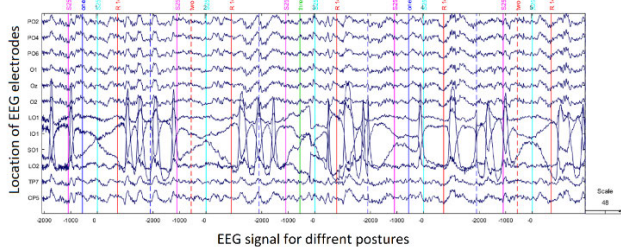


FIGURE 12. EEG for different postures with the placement of electrodes from CP5 to PO2.

In the proposed system, EEG analysis is carried out using realistic head models to identify the unique EEG signal features and to validate the brain network connectivity. Here, a 64-electrode placement scheme is used in the proposed system. The electrodes are placed in the frontal and parietal

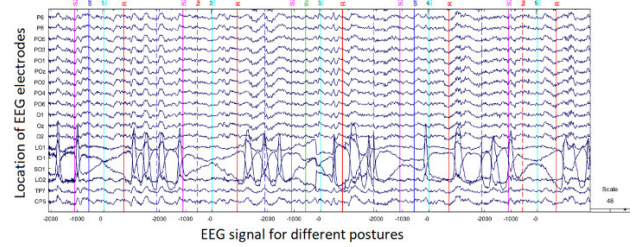


FIGURE 13. EEG for different postures with the placement of electrodes from CP5 to P6.

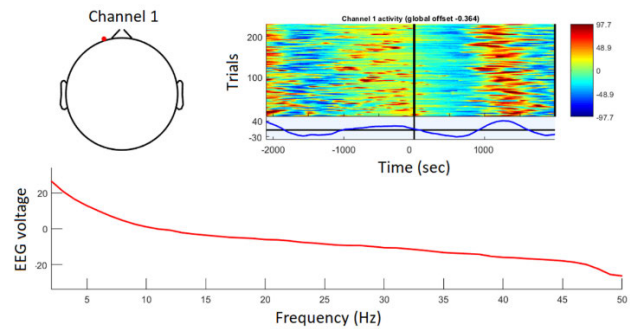


FIGURE 14. EEG voltage for different frequency and number of trials per second.

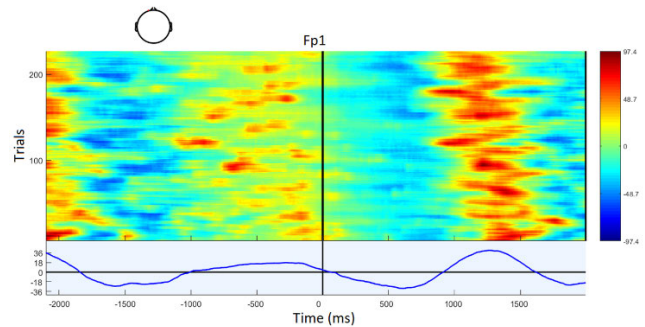


FIGURE 15. Number of trials with time.

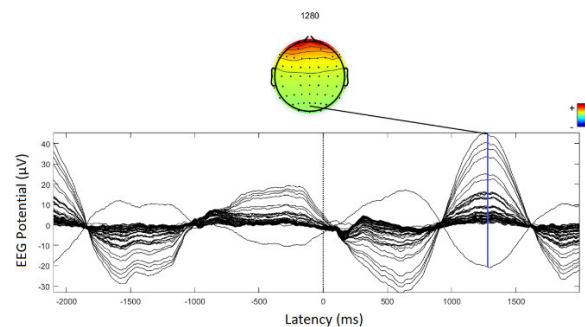


FIGURE 16. EEG voltage for different frequency and number of trails per second.

regions of the brain. Figure 10 indicates the electrode placement positions used for testing the proposed system.

Figure 11 shows the EEG signal for different postures with the placement of electrodes from positions CP5 to LO1,

and figure 12 shows the EEG for different postures with the placement of electrodes from CP5 to PO2 positions and figure 13 shows the EEG for different postures with the placement of electrodes from CP5 to P6 positions. Figure 14 shows the EEG voltage for different frequencies and also the number of trials per second.

Figure 15 shows the number of trials carried out with time, and figure 16 shows the EEG potential with varying latency using the proposed system. The proposed system achieves excellent performance in all real-time scenarios. Results confirm that the proposed method provides adequate assistance and rehabilitation for paralyzed patients.

## V. CONCLUSION

To overcome the constraints of weight, flexibility, and adaptability faced by the existing exoskeletons used for assisting the paralyzed people, we proposed an adaptive and flexible Brain Energized Full Body Exoskeleton (BFBE). The brain signals captured by the EEG sensors are used for controlling the movements of the exoskeleton. The flexibility is incorporated into the system by a modular design approach. The parts and joints can be attached and detached easily, allowing it to be used by people with different levels of paralysis. For the fully paralyzed, the full-body exoskeleton structure can be used. The processing happens at the edge, thus reducing delay in decision making, and the system is further integrated with an IoT module that helps to send an alert message to multiple caregivers in case of an emergency. The potential energy harvesting is used in the system to solve the power issues related to the exoskeleton. The stability in the gait cycle is ensured by using adaptive sensory feedback. The system was by using six natural movements on ten different paralyzed persons and received very good results.

## REFERENCES

- [1] Multiple Sclerosis News Today. *Mobility Devices for Lower-Limb Paralysis Flawed, Survey Reveals*. Accessed: Jun. 20, 2019. [Online]. Available: <https://multiplesclerosisnewstoday.com/2018/06/08/mobility-devices-lower-limb-paralysis-flawed-survey>
- [2] S. Alqahtani, J. Joseph, B. Dicianno, N. A. Layton, M. L. Toro, E. Ferretti, Y. A. Tuakli-Wosornu, H. Chhabra, H. Neyedli, C. R. Lopes, M. M. Alqahtani, P. Van de Vliet, S.-I. Kumagaya, J.-B. Kim, V. McKinney, Y.-S. Yang, M. Goldberg, and R. Cooper, "Stakeholder perspectives on research and development priorities for mobility assistive-technology: A literature review," *Disab. Rehabil. Assistive Technol.*, pp. 1–15, Dec. 2019, doi: [10.1080/17483107.2019.1650300](https://doi.org/10.1080/17483107.2019.1650300).
- [3] D. Ao, R. Song, and J. Gao, "Movement performance of human-robot cooperation control based on EMG-driven hill-type and proportional models for an ankle power-assist exoskeleton robot," *IEEE Trans. Neural Syst. Rehabil. Eng.*, vol. 25, no. 8, pp. 1125–1134, Aug. 2017, doi: [10.1109/TNSRE.2016.2583464](https://doi.org/10.1109/TNSRE.2016.2583464).
- [4] Q. Ma, L. Ji, and R. Wang, "The development and preliminary test of a powered alternately walking exoskeleton with the wheeled foot for paraplegic patients," *IEEE Trans. Neural Syst. Rehabil. Eng.*, vol. 26, no. 2, pp. 451–459, Feb. 2018.
- [5] T. Zhang, M. Tran, and H. Huang, "Design and experimental verification of hip exoskeleton with balance capacities for walking assistance," *IEEE/ASME Trans. Mechatronics*, vol. 23, no. 1, pp. 274–285, Feb. 2018, doi: [10.1109/TMECH.2018.2790358](https://doi.org/10.1109/TMECH.2018.2790358).
- [6] J. C. Perry, J. Rosen, and S. Burns, "Upper-limb powered exoskeleton design," *IEEE/ASME Trans. Mechatronics*, vol. 12, no. 4, pp. 408–417, Aug. 2007, doi: [10.1109/TMECH.2007.901934](https://doi.org/10.1109/TMECH.2007.901934).
- [7] A. Sutrisno and D. J. Braun, "Enhancing mobility with quasi-passive variable stiffness exoskeletons," *IEEE Trans. Neural Syst. Rehabil. Eng.*, vol. 27, no. 3, pp. 487–496, Mar. 2019, doi: [10.1109/TNSRE.2019.2899753](https://doi.org/10.1109/TNSRE.2019.2899753).
- [8] P. G. Vinoj, S. Jacob, V. G. Menon, S. Rajesh, and M. R. Khosravi, "Brain-controlled adaptive lower limb exoskeleton for rehabilitation of post-stroke paralyzed," *IEEE Access*, vol. 7, pp. 132628–132648, 2019, doi: [10.1109/access.2019.2921375](https://doi.org/10.1109/access.2019.2921375).
- [9] M. Sarac, M. Solazzi, and A. Frisoli, "Design requirements of generic hand exoskeletons and survey of hand exoskeletons for rehabilitation, assistive, or haptic use," *IEEE Trans. Haptics*, vol. 12, no. 4, pp. 400–413, Oct. 2019, doi: [10.1109/toh.2019.2924881](https://doi.org/10.1109/toh.2019.2924881).
- [10] F. Patane, S. Rossi, F. D. Sette, J. Taborri, and P. Cappa, "WAKE-up exoskeleton to assist children with cerebral palsy: Design and preliminary evaluation in level walking," *IEEE Trans. Neural Syst. Rehabil. Eng.*, vol. 25, no. 7, pp. 906–916, Jul. 2017, doi: [10.1109/tnsre.2017.2651404](https://doi.org/10.1109/tnsre.2017.2651404).
- [11] H.-J. Lee, S. Lee, W. H. Chang, K. Seo, Y. Shim, B.-O. Choi, G.-H. Ryu, and Y.-H. Kim, "A wearable hip assist robot can improve gait function and cardiopulmonary metabolic efficiency in elderly adults," *IEEE Trans. Neural Syst. Rehabil. Eng.*, vol. 25, no. 9, pp. 1549–1557, Sep. 2017, doi: [10.1109/tnsre.2017.2664801](https://doi.org/10.1109/tnsre.2017.2664801).
- [12] A. Agrawal, O. Harib, A. Hereid, S. Finet, M. Masselin, L. Praly, A. D. Ames, K. Sreenath, and J. W. Grizzle, "First steps towards translating HZD control of bipedal robots to decentralized control of exoskeletons," *IEEE Access*, vol. 5, pp. 9919–9934, 2017, doi: [10.1109/access.2017.2690407](https://doi.org/10.1109/access.2017.2690407).
- [13] M. K. Shepherd and E. J. Rouse, "Design and validation of a torque-controllable knee exoskeleton for Sit-to-Stand assistance," *IEEE/ASME Trans. Mechatronics*, vol. 22, no. 4, pp. 1695–1704, Aug. 2017, doi: [10.1109/tmech.2017.2704521](https://doi.org/10.1109/tmech.2017.2704521).
- [14] M. Cenciari and M. A. Dollar, "Biomechanical considerations in the design of lower limb exoskeletons," in *Proc. IEEE Int. Conf. Rehabil. Robot.*, Zürich, Switzerland, Jun./Jul. 2011, pp. 1–6, doi: [10.1109/ICORR.2011.5975366](https://doi.org/10.1109/ICORR.2011.5975366).
- [15] H. Herr, "Exoskeletons and orthoses: Classification, design challenges and future directions," *J. NeuroEng. Rehabil.*, vol. 6, no. 1, p. 21, Dec. 2009, doi: [10.1186/1743-0003-6-21](https://doi.org/10.1186/1743-0003-6-21).
- [16] A. Agrawal, A. N. Dube, D. Kansara, S. Shah, and S. Sheth, "Exoskeleton: The friend of mankind in context of rehabilitation and enhancement," *Indian J. Sci. Technol.*, vol. 9, no. S1, pp. 1–8, Dec. 2016, doi: [10.17485/ijst/2016/v9is1/100889](https://doi.org/10.17485/ijst/2016/v9is1/100889).
- [17] C. Chen, X. Wu, D.-X. Liu, W. Feng, and C. Wang, "Design and voluntary motion intention estimation of a novel wearable full-body flexible exoskeleton robot," *Mobile Inf. Syst.*, vol. 2017, pp. 1–11, Jun. 2017, doi: [10.1155/2017/8682168](https://doi.org/10.1155/2017/8682168).
- [18] A. Singla, S. Dhand, A. Dhawad, and G. S. Virk, "Toward human-powered lower limb exoskeletons: A review," in *Harmony Search and Nature Inspired Optimization Algorithms. Advances in Intelligent Systems and Computing*, vol. 741. Singapore: Springer, 2019, pp. 783–795, doi: [10.1007/978-981-13-0761-4\\_75](https://doi.org/10.1007/978-981-13-0761-4_75).
- [19] S. Federici, F. Meloni, M. Bracalenti, and M. L. De Filippis, "The effectiveness of powered, active lower limb exoskeletons in neurorehabilitation: A systematic review," *NeuroRehabilitation*, vol. 37, no. 3, pp. 321–340, Nov. 2015, doi: [10.3233/nre-151265](https://doi.org/10.3233/nre-151265).
- [20] G. Menga and M. Ghirardi, "Lower limb exoskeleton for rehabilitation with improved postural equilibrium," *Robotics*, vol. 7, no. 2, p. 28, Jun. 2018, doi: [10.3390/robotics7020028](https://doi.org/10.3390/robotics7020028).
- [21] H. Kazerooni and R. Steger, "The berkeley lower extremity exoskeleton," *J. Dyn. Syst., Meas., Control*, vol. 128, no. 1, pp. 14–25, Mar. 2006, doi: [10.1115/1.2168164](https://doi.org/10.1115/1.2168164).
- [22] V. G. Menon, S. Jacob, S. Joseph, and A. O. Almagrabi, "SDN powered humanoid with edge computing for assisting paralyzed patients," *IEEE Internet Things J.*, early access, Dec. 2019, doi: [10.1109/JIOT.2019.2963288](https://doi.org/10.1109/JIOT.2019.2963288).
- [23] S. Jacob, V. G. Menon, F. Al-Turjman, V. P. G., and L. Mostarda, "Artificial muscle intelligence system with deep learning for post-stroke assistance and rehabilitation," *IEEE Access*, vol. 7, pp. 133463–133473, 2019, doi: [10.1109/ACCESS.2019.2941491](https://doi.org/10.1109/ACCESS.2019.2941491).

- [24] L. Jiang, A. Stocco, D. M. Losey, J. A. Abernethy, C. S. Prat, and R. P. N. Rao, "BrainNet: A multi-person brain-to-brain interface for direct collaboration between brains," *Sci. Rep.*, vol. 9, no. 1, pp. 1–11, Dec. 2019, doi: [10.1038/s41598-019-41895-7](https://doi.org/10.1038/s41598-019-41895-7).
- [25] W. Lee, S. Kim, B. Kim, C. Lee, Y. A. Chung, L. Kim, and S.-S. Yoo, "Non-invasive transmission of sensorimotor information in humans using an EEG/focused ultrasound brain-to-brain interface," *PLoS ONE*, vol. 12, no. 6, Jun. 2017, Art. no. e0178476, doi: [10.1371/journal.pone.0178476](https://doi.org/10.1371/journal.pone.0178476).
- [26] S. Rajesh, V. Paul, V. G. Menon, S. Jacob, and P. Vinod, "Secure brain-to-brain communication with edge computing for assisting post-stroke paralyzed patients," *IEEE Internet Things J.*, vol. 7, no. 4, pp. 2531–2538, Apr. 2020, doi: [10.1109/JIOT.2019.2951405](https://doi.org/10.1109/JIOT.2019.2951405).



**SUNIL JACOB** (Member, IEEE) received the Ph.D. degree in electronics and communication engineering from Bharathiar University, India, in 2015. He is currently the Director with the Centre for Robotics and a Professor with the Department of Electronics and Communication Engineering, SCMS School of Engineering and Technology, India. He is also doing postdoctoral research with the Lincoln University College, Malaysia. His project Muscles to Machine Interface for Paralyzed has been funded by the IEEE EPICS, USA, and other funded projects include bionic haptic arm, rejuvenating the cells of human body, deaddiction coil for drug addicts, smart keyboard for disabled person, low cost 3-D printer, and wearable device for detection and prevention of heart failure. He was a recipient of the AICTE Chhatra Vishwakarma Award, in electronics, in 2017, and the Young Gandhian Technological Innovation Appreciation Award, in 2018.



**MUKIL ALAGIRISAMY** received the bachelor's degree in electronics and communication engineering, the M.Eng. degree in communication systems, and the Ph.D. degree in engineering, in 2005, 2007, and 2012, respectively. She completed her PDF, in 2015. She started her career as a Lecturer with the Hindustan Engineering College, India. She was working as an Assistant Professor with B. S. Abdur Rahman University, India. Later, she joined the Stamford College, Malaysia, as a Lecturer. She is currently an Associate Professor with the Department of Electrical and Electronics and Engineering, Lincoln University College, Malaysia. She is also working as an Assistant Professor and a Coordinator of the Master of Science in Electrical, Electronics and Telecommunication Engineering Programs, Lincoln University College. She has 12 years of experience in teaching subjects like data communication, analog and digital communications, digital signal processing, and satellite communications. Her research interests include sink mobility patterns, clustering, modulation, data aggregation, and compressive sensing techniques for wireless sensor networks.



**VARUN G. MENON** (Senior Member, IEEE) received the Ph.D. degree in computer science and engineering from Sathyabama University, India, in 2017. He is currently an Associate Professor with the Department of Computer Science and Engineering, SCMS School of Engineering and Technology, India. His research interests include sensors, the Internet of Things (IoT), fog computing, and underwater acoustic sensor networks. He is also serving as the Guest Editor for the IEEE

*Sensors Journal*, the IEEE Internet of Things Magazine, and the IEEE TRANSACTIONS ON INDUSTRIAL INFORMATICS. He is an Associate Editor of IET Quantum Communications and also an Editorial Board Member of IEEE Future Directions: Technology Policy and Ethics. He is also a Distinguished Speaker of ACM.



**B. MANOJ KUMAR** received the Ph.D. degree in mechanical engineering from Karpagam University, India. He is currently an Associate Professor and the Head of the Department of Automobile Engineering, SCMS School of Engineering and Technology, India. His research interests include sensor networks and industrial engineering.



**N. Z. JHANJHI** is currently working as an Associate Professor with Taylor's University, Malaysia. He has great international exposure in academia, research, administration, and academic quality accreditation. He worked with Ilma University and King Faisal University (KFU), Saudi Arabia, for a decade. He has 20 years of teaching and administrative experience. He has an intensive background of academic quality accreditation in higher education. Besides scientific research activities,

he had worked a decade for academic accreditation and earned ABET accreditation twice for three programs at CCSIT, KFU. He also worked for the National Commission for Academic Accreditation and Assessment (NCAAA), the Education Evaluation Commission Higher Education Sector (EECHES), formerly NCAAA, Saudi Arabia, for institutional level accreditation. He also worked for the National Computing Education Accreditation Council (NCEAC). He was awarded as a top Reviewer 1% globally by WoS/ISI (Publons) recently for the year 2019. He has edited or authored more than 13 research books with international reputed publishers, earned several research grants, and a great number of indexed research articles on his credit. He has supervised several postgraduate students, including the master's and Ph.D. students. He is an Associate Editor of the IEEE Access, a Moderator of the IEEE TechRxiv, a keynote speaker for several IEEE international conferences globally, an External Examiner or an Evaluator for Ph.D. and master's students for several universities, a Guest editor of several reputed journals, a member of the editorial board of several research journals, and an active TPC Member of reputed conferences around the globe.



**VASAKI PONNUSAMY** received the bachelor's and M.Sc. degrees in computer science from the University of Science, Malaysia, and the Ph.D. degree in IT from Universiti Teknologi PETRONAS (UTP), Malaysia, in 2013. She is currently an Assistant Professor with Universiti Tunku Abdul Rahman, Malaysia. She is also the Head of the Department of Computer and Communication Technology, Faculty of Information and Communication Technology. She is also working

on cybersecurity, the Internet-of-Things (IoT) security trends, and digital governance. She has great international exposure as a Keynote Speaker, a Visiting Professor, and several Fellowships. She has edited or authored several research books with international reputed publishers, earned several research grants, and supervising postgraduate students. She is also a Human Resource Development Fund Certified Trainer and a Master Trainer for computational thinking and computer science teaching. Her career in academia started, in 1999. She has been teaching information and network security, wireless security, and data communication and networking. She is specialized in handling Cisco devices for routing and security. Her passion is to share her technical knowledge with the community. Her area of specializations are networking, communication, penetration testing, and cybersecurity. She has worked on several projects on IoT intrusion detection systems, cybersecurity governance, social engineering attacks mitigation/awareness, and human behavior-based authentication systems.



include deep learning, cloud security and privacy, *ad hoc* networks, and big data.

**P. G. SHYNU** received the Ph.D. degree in computer science from the Vellore Institute of Technology (VIT), Vellore, India, and the master's degree in computer science and engineering from the College of Engineering, Anna University, Chennai, India. He is currently working as an Associate Professor with the School of Information Technology and Engineering, VIT. He has published over 30 research papers in refereed international conferences and journals. His research interests



applications. He is the Founder of Anidra Tech Ventures Pty Ltd., a smart remote patient monitoring company. He contributed immensely to eResearch software research and development that uses cloud-based infrastructure and a core member for the project sponsored by Nectar Australian research cloud provider. He contributed heavily in the field of healthcare informatics, sensor networks, and cloud computing.

**VENKI BALASUBRAMANIAN** (Member, IEEE) received the Ph.D. degree in body area wireless sensor network (BAWSN) for remote healthcare monitoring applications. He is the Pioneer in building (pilot) remote healthcare monitoring application (rHMA) for pregnant women for the New South Wales Healthcare Department. His research establishes a dependability measure to evaluate rHMA that uses BAWSN. His research opens up a new research area in measuring time-critical

• • •